The FEBS Journal

FEBS PRESS science publishing by scientists

RFTS-dependent negative regulation of Dnmt1 by nucleosome structure and histone tails

Yuichi Mishima[1,*], Laura Brueckner[1,*], Saori Takahashi[1], Toru Kawakami[2], Kyohei Arita[3], Shota Oka[1], Junji Otani[1], Hironobu Hojo[2], Masahiro Shirakawa[4,5], Akira Shinohara[6], Mikio Watanabe[7] and Isao Suetake[1,5,7,8,*]

1 Laboratory of Epigenetics, Institute for Protein Research, Osaka University, Suita, Japan
2 Laboratory of Organic Chemistry, Institute for Protein Research, Osaka University, Suita, Japan
3 Division of Macromolecular Crystallography, Graduate School of Nanobioscience, Yokohama City University, Japan
4 Department of Molecular Engineering, Graduate School of Engineering, Kyoto University, Japan
5 CREST, Japan Science and Technology Agency, Saitama, Japan
6 Laboratory of Genome-Chromosome Functions, Institute for Protein Research, Osaka University, Suita, Japan
7 Center for Twin Research, Graduate School of Medicine, Osaka University, Suita, Japan
8 College of Nutrition, Koshien University, Takarazuka, Japan

Keywords
Dnmt1; histone; modifications; nucleosomes; replication foci targeting sequence

Correspondence
Y. Mishima and I. Suetake, Institute for Protein Research, Osaka University, 3-2 Yamadaoka, Suita, Osaka, Japan
Fax: +81 6 6879 8603
Tel: +81 6 6879 8628
E-mails: mishima@protein.osaka-u.ac.jp (YM) and hotsuetake@hotmail.com (IS)

*Equally contributed

(Received 30 March 2017, revised 7 July 2017, accepted 17 August 2017)

doi:10.1111/febs.14205

DNA methylation in promoter regions represses gene expression and is copied over mitotic divisions by Dnmt1. Dnmt1 activity is regulated by its replication foci targeting sequence (RFTS) domain which masks the catalytic pocket. It has been shown that Dnmt1 activity on unmethylated DNA is inhibited in nucleosome cores. In the present study, we aimed to assess the effect of nuclesome formation on maintenance methylation at single CpG resolution. We show that Dnmt1 fully methylates naked linker DNA in dinucleosomes, whereas maintenance methylation was repressed at all CpG sites in nucleosome core particles. Deletion of RFTS partly released obstruction of Dnmt1 activity in core particles. Histone H3 tail peptides inhibited Dnmt1 in an RFTS-dependent manner and repression was modulated by acetylation or methylation. We propose a novel function of RFTS to regulate Dnmt1 activity in nucleosomes.

Introduction

The 5th position of genomic Cytosine is frequently methylated. In gene promoters, methylation represses transcription, whereas there is a positive correlation with expression when methylation is located in gene bodies [1]. DNA methylation is crucial for normal development [2]. Once DNA methylation patterns are established, they are faithfully maintained through cell divisions. Maintenance DNA methylation is essential not only for differentiated cells but also for epigenetic reprogramming from primed to naïve pluripotent cells [3]. When maintenance methylation is impaired, aberrantly differentiated or apoptotic cells are observed [4,5]. Despite numerous analyses of methylation patterns, the regulatory mechanism of DNA methylation is still largely unknown.

Dnmt1 is the enzyme primarily responsible for the accurate perpetuation of DNA methylation patterns following cell division. It can target unmethylated

Abbreviation
Dnmt1, DNA methyltransferase 1; λ exo, λ exonuclease.

DNA but has a preference for hemimethylated substrate [6,7]. Dnmt1$^{-/-}$ knockout in mice is lethal at early embryonic stage [8]. Dnmt1 is a multidomain protein [9,10], containing an independent replication foci targeting sequence (RFTS) domain. RFTS masks the catalytic pocket, and this intramolecular interaction increases the activation energy of Dnmt1 [9]. Dnmt1 interacts directly and/or indirectly with histone tail regions. In egg or cell lysate, the RFTS domain binds to ubiquitin, ubiquitylated histone H3, and unmodified H3 [11–13]. However, the physiological meaning of the interaction between RFTS and histone H3 is unclear.

The direct effect of nucleosomal structure on Dnmt1 activity *in vitro* has been reported in several studies, however, the described effects are controversial. The maximal activity of Dnmt1 toward mononucleosomes reconstituted with unmethylated DNA and histones prepared from HeLa cells was unchanged compared to naked DNA but K_m values on substrates were increased by nucleosome structure [14]. When mononucleosomes were reconstituted with recombinant histones and unmethylated DNA, Dnmt1 activity toward nucleosomes was slightly reduced compared to naked DNA [15]. In another study, mononucleosomes including some hemimethylated CpG sites were used. DNMT1 showed an intrinsic ability to methylate CpG sites packaged into nucleosomes but the activity was DNA sequence dependent [16]. Analysis of mononucleosomes with unmethylated DNA by bisulfite sequencing showed that Dnmt1 *de novo* methylation was inhibited in nucleosome cores but not on linker DNA. Dnmt1 activity toward hemimethylated nucleosomal arrays was also reported to be lower than that toward naked DNA [17].

Dnmt1 methylates hemimethylated DNA in a processive manner, whereas unmethylated substrate is modified distributively [7]. In the present study, we therefore specifically address the effect of nucleosome structure on Dnmt1 maintenance methylation activity by using reconstituted dinucleosomes in which all CpG sites are hemimethylated. Using bisulfite sequencing, we mapped Dnmt1 activity at single CpG resolution. As previously shown for *de novo* methylation [17], core regions in the nucleosomes were refractory to maintenance methylation while linker DNA was not. On naked DNA, histone tail peptides repressed Dnmt1 activity at low micromolar concentration. This repression was lost upon removal of the RFTS domain. Acetylation of histone H3 peptide abolished interaction with RFTS and Dnmt1 inhibition. Our results suggest that histone presence regulates Dnmt1 maintenance methylation activity in two ways. Firstly, nucleosomes obstruct Dnmt1 access to DNA and this steric hindrance is partially released by RFTS removal. Secondly, the interaction with unmodified histone tails can inhibit Dnmt1 activity directly by stabilizing RFTS-dependent autoinhibition.

Results

Repression of the methylation activity of Dnmt1 in the nucleosome core region

At single base resolution, analysis of Dnmt1-catalyzed methylation has so far been performed on nucleosomes prepared with unmethylated DNA [17]. To elucidate the effect of nucleosomal structure on mouse Dnmt1 activity on its intrinsic target, we prepared high-purity hemimethylated DNA which can be analyzed by sodium bisulfite sequencing (Fig. 1A). More than 95% of CpG sites on the upper strand in purified hemimethylated DNA were methylated, while less than 5% of CpG sites on the lower strand were sporadically methylated (Fig. 1B). The N-terminal 290 amino acids of Dnmt1 contain a sequence which binds to PCNA

Fig. 1. Preparation of hemimethylated DNA and maintenance methylation activity by Dnmt1 291. (A) Preparation of hemimethylated DNA. Schematically illustrated procedure of hemimethylated DNA preparation (left panel). Methylated cytosine in CpG sequences is indicated by red circles. DNA for each step was separated in 5% native PAGE, and fluorescently detected (right panel). PCR product, with a length of 570 bp, (lane 1) was methylated with M. SssI, and then treated with λexo. After λexo treatment, two bands (lane 2), which are derived from double- (570 bp DNA) and single-stranded DNA (arrowhead), were detected. The contaminating double-stranded DNA was removed with an acrylamide disk gel (lane 3), and then the lower strand was filled in using T4 polymerase (lane 4). The DNA was digested with *Bam*HI and *Hin*dIII (lane 5), and the product was purified with an acrylamide disk gel (lane 6). The samples were run on the same gel, but intervening lanes were removed. The splice site is indicated by a black vertical line in the figure. DNA sequences of the primers are shown in Table S3. (B) Confirmation of methylation status of hemimethylated DNA. After bisulfite treatment, DNA was amplified with specific primers. The amplified DNA was subcloned and sequenced. Methylated and unmodified cytosines in upper strand (left panel) and lower strand (right panel) are indicated by closed and open circles, respectively. Nucleosomal positioning sites are shown at the top of the panel. CpG site numbers, as designated in Fig. S1, are shown at the bottom of panel. (C) Methylation status on naked DNA. Methylated and unmodified cytosines are indicated with closed and open circles, respectively.

during replication. Dnmt1 291 lacking this domain is functionally similar to full-length Dnmt1 *in vivo* [18] and in terms of enzymatic activity on naked DNA [6].

At first we analyzed the methylation activity of Dnmt1 291 on naked hemimethylated DNA. More than 90% of CpG sites were methylated by Dnmt1 291 and we

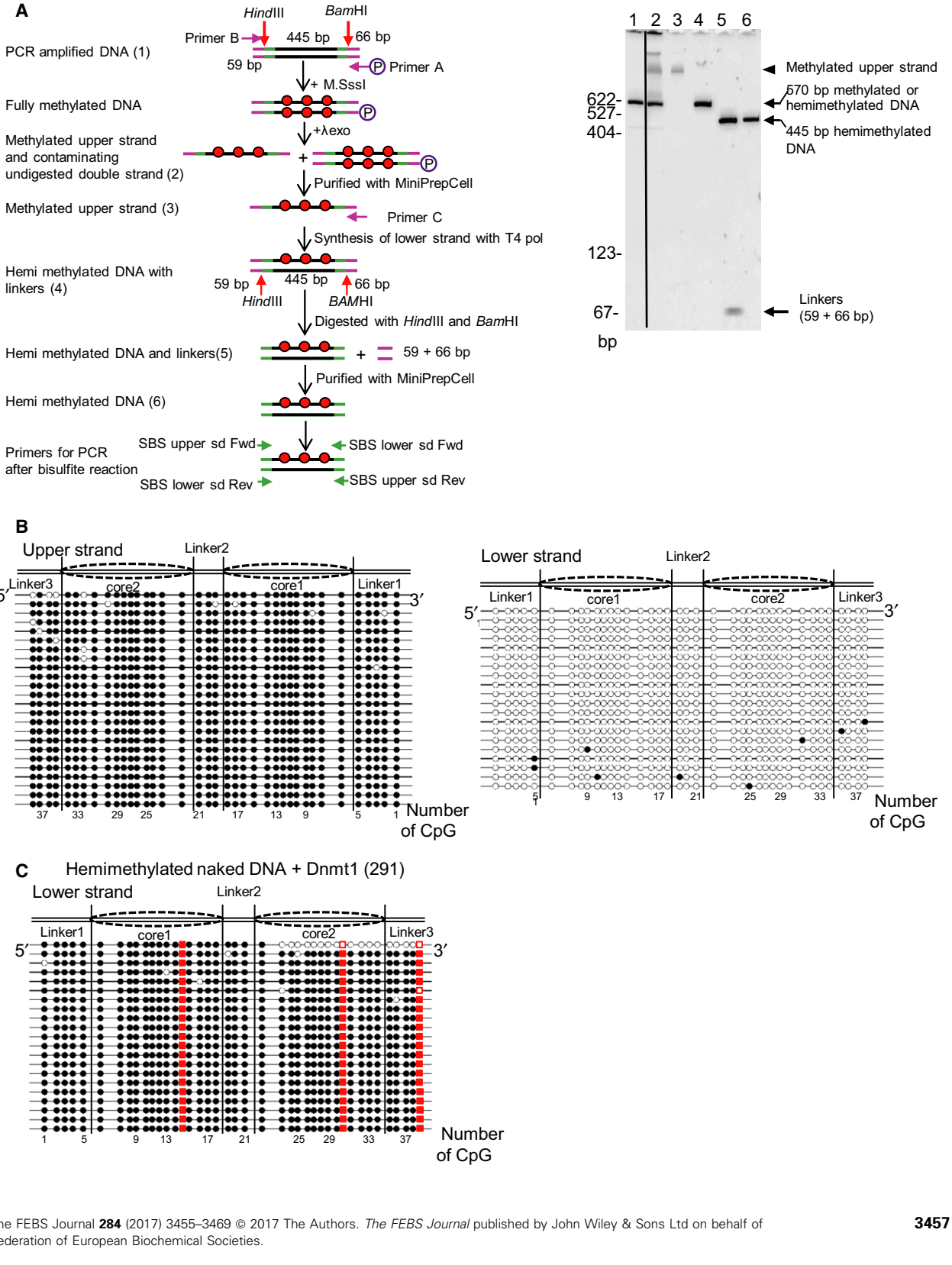

did not observe specific sites exempt from methylation (Fig. 1C), indicating that all CpG sites are recognized by Dnmt1 291 in equal manner.

We then reconstituted dinucleosomes from hemimethylated DNA and recombinant histones. In the nucleosomes, contamination by free DNA was negligible (Fig. 2A), nucleosome core particles were positioned as expected (Fig. 2B), and the size of DNA wrapped on the core particles was similar to unmethylated template (Fig. 2C). The prepared nucleosomes were then used in a methylation reaction with Dnmt1 291 (Fig. 2D). To monitor the integrity of the nucleosomes during the reaction, bacterial methyltransferase M. AluI was added [19]. In three independent experiments, CpG sites in both core particle regions core 1 (CpG number 6–18) and core 2 (CpG 22–34) were scarcely methylated, while more than 90% of CpG sites in all linker DNA regions (linkers 1, 2, and 3) were methylated (Fig. 2E and Fig. S2).

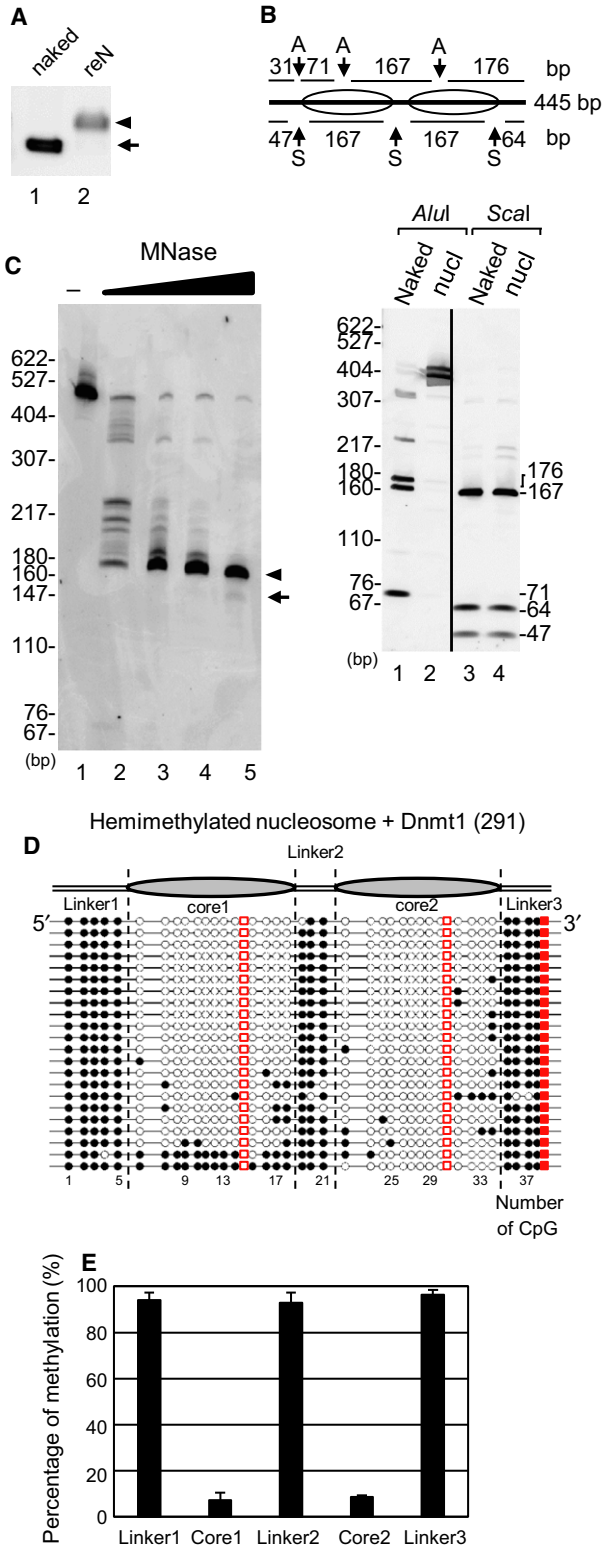

Fig. 2. Reconstitution of hemimethylated dinucleosomes and susceptibility for DNA methylation by Dnmt1 291. (A) Hemimethylated naked DNA and dinucleosomes (reN) were visualized by electrophoresis on a 0.7% agarose gel. The positions of dinucleosomes reconstituted with hemimethylated DNA (lane 2) (arrowhead) and naked DNA (lane 1, arrow) bands are indicated. (B) Restriction enzyme susceptibility of the reconstituted dinucleosomes. Schematic illustration of the reconstituted nucleosomes (upper panel). The positions of the restriction enzymes, *AluI* (A) and *ScaI* (S), and the expected location of the histone octamer (dotted line ellipse) are indicated. The sizes (bp) of the digested DNA are shown. The positions of nucleosome cores in dinucleosomes were monitored by digestion with restriction enzymes, by using *AluI* and *ScaI*, as described [41]. Naked DNA (lanes 1 and 3) and nucleosomes (lanes 2 and 4) were treated with *AluI* (lanes 1 and 2) or *ScaI* (lanes 3 and 4), and then separated in 5% native PAGE. The samples were run on the same gel, but the intervening lanes were removed. The splice site is indicated by a black vertical line in the figure. Size markers (in base pairs) are indicated at the left of the panel. (C) Micrococcal nuclease (MNase) susceptibility of the hemimethylated dinuclesomes. Dinucleosomes were treated with MNase (3 U·mL^{-1} for lane 2; 9 U·mL^{-1} for lane 3; 27 U·mL^{-1} for lane 4; and 89 U·mL^{-1} for lanes 5) or without MNase (lane 1). The positions of the 160 bp (arrowhead) and 146 bp (arrow) bands that were protected from MNase digestion are indicated. (D) Methylation status on nucleosomal DNA-methylated by Dnmt1 (291). Methylated and unmodified cytosines are indicated with closed and open circles, respectively. The margins between linker DNA and nucleosome core region are indicated by dotted lines. The experiment was repeated and the results are shown in Fig. S2. Methylated and unmodified cytosines in M. AluI recognition sites, 5′-AGCT-3′, are indicated by closed and open red rectangles, respectively. Bisulfite sequencing data in which destabilization of nucleosome structure was observed via M. AluI methylation was omitted. (E) Region-specific methylation on the reconstituted dinucleosomes. Percentage of methylated CpG in each region is shown in bar plot as average of three independent experiments (data from panel D and Fig. S2).

Full-length Dnmt1 (Dnmt1 FL), as well as Dnmt1 291, methylated more than 90% of CpG sites in the naked hemimethylated DNA (compare Fig. 3A and 1C). The prepared nucleosomes were then methylated with Dnmt1 FL (Fig. 3B). CpG sites in both core 1 and core 2 were scarcely methylated, while more than 90% of CpG sites in all linker DNA regions were methylated (Figs 3C and S3). The methylation pattern introduced by Dnmt1 FL was comparable to that by Dnmt1 291 (compare Figs 3C and 2E). In addition, no significant difference between the percentage of DNA methylation in each CpG catalyzed by Dnmt1 FL and Dnmt1 291 was observed (Fig. 3D). These suggest that the N-terminal region (amino acids 1–290) does not contribute to Dnmt1 inhibition by nucleosome structure.

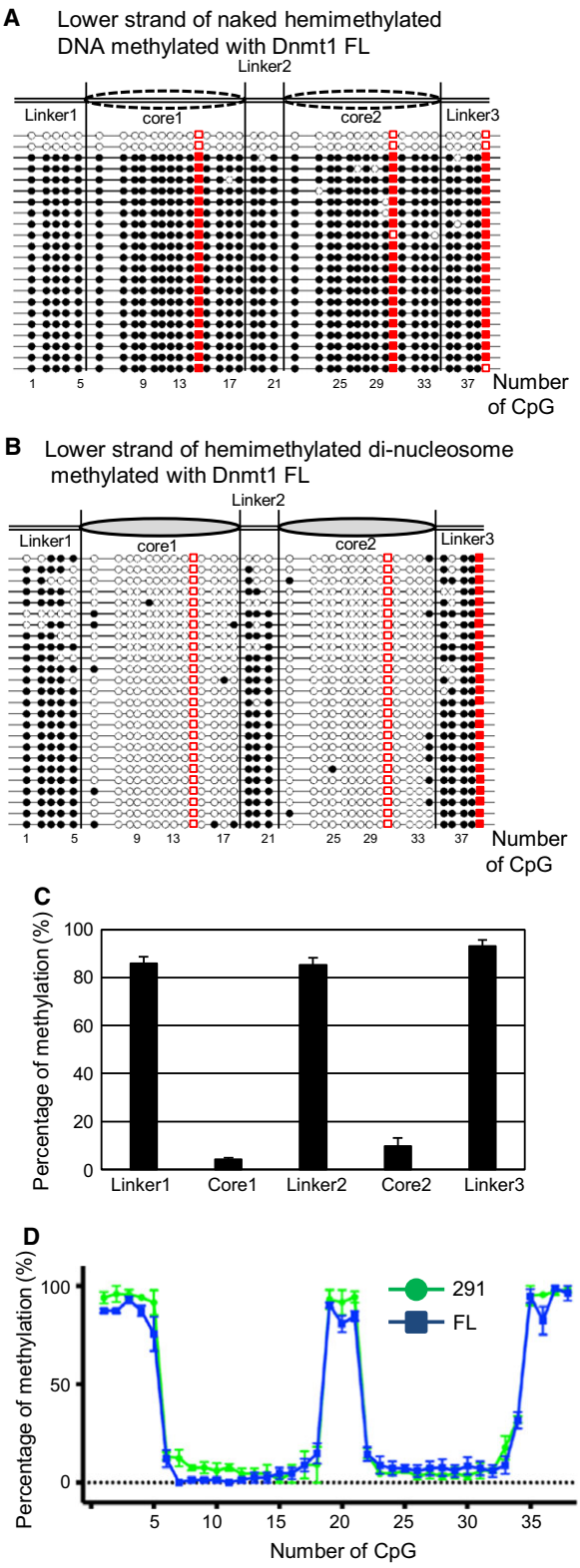

Fig. 3. Nucleosome structure-dependent DNA methylation activity of Dnmt1 FL. Hemimethylated naked DNA (A) or dinucleosomes (B) were methylated by Dnmt1 FL. Two additional independent experiments were performed, and shown in Fig. S3. (C) Percentage of CpG methylation in the regions (linker 1, 2, 3, and core 1, 2) was shown as average ± SD ($n = 3$) (data from panel B and Fig. S3), as Fig. 2E. (D) Single-base analysis of DNA methylation. The percentage of DNA methylation in each CpG was plotted to the DNA sequence. Dinucleosomes were methylated with Dnmt1 291 (green line) or Dnmt1 FL (blue line) The percentage ± SD ($n = 3$) is shown. The data are derived from Figs 2D and S2 (Dnmt1 291), panel B and Fig. S3 (Dnmt1 FL).

Increase in Dnmt1 access to nucleosome entry/exit sites by removing RFTS

In *Xenopus* egg lysate, the N-terminal region (amino acids 180–470) lacking the PCNA binding domain but including the RFTS region of *Xenopus* Dnmt1 has been reported to bind to unmodified histone H3 [13]. We also detected binding of GST-mouse Dnmt1 to the N-terminal region of histone H3 (amino acids 1–30) which is limited to the RFTS domain (amino acids 291–602) (Fig. 4A). Crystal structure suggests that RFTS interacts with the catalytic pocket to block access to substrate DNA (Fig. 4B), thereby increasing activation energy [9]. We examined whether the truncation of RFTS changes the inhibitory effect of nucleosomes, by preparing Dnmt1 with a deletion of amino acids 1–601 (Dnmt1 602) (Fig. 4C). As for Dnmt1 291, we observed that the methylation activity of Dnmt1 602 was repressed by nucleosome structure (Figs 4D, S4, and 5A). The percentage of methylated CpGs in core regions methylated with Dnmt1 602 was slightly higher compared to Dnmt1 291 (compare Fig. 5A and 2E). On closer inspection, methylation in the central region of the nucleosome cores was unchanged, while in the marginal regions close to the entry/exit sites of both nucleosome cores methylation

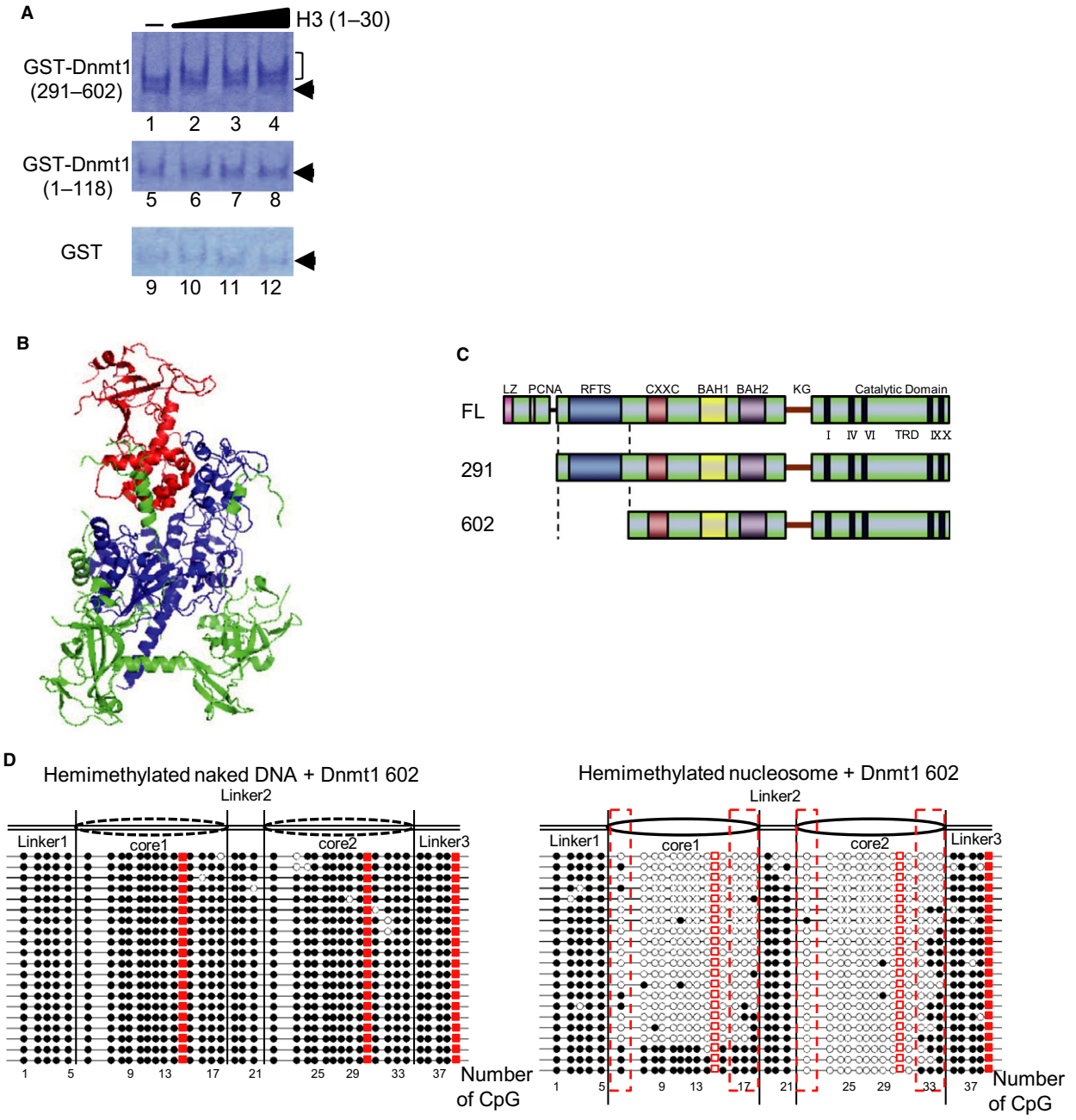

Fig. 4. Binding of Dnmt1 N-terminal region to histone H3 tail and effect of nucleosome structure on the Dnmt1 601 activity. (A) Interaction between histone H3 (1–30) and N-terminal regions of Dnmt1. Recombinant GST-tagged (291–601) (lanes 1–4), GST-Dnmt1 (1–118) (lanes 5–8), or GST (lanes 9–12) were mixed with 5.6× (lanes 2, 6, and 10), 17× (lanes 3, 7, and 11), and 56× (lanes 4, 8, and 12) molar excess of histone H3 (1–30) or no histone H3 (lanes 1, 5, and 9), and separated in 6% native acrylamide gel. Arrows and bracket indicate the unbound and bound band, respectively. (B) Structure of Dnmt1. RFTS domain and catalytic domain of Dnmt1 (PDB: 3AV4) are indicated by red and blue, respectively. (C) Schematic illustration of truncated Dnmt1. (D) Methylation status of naked DNA (left panel) and nucleosomes (right panel) methylated with Dnmt1 602.

was increased (Fig. 5B). Both Dnmt1 291 and 601 methylated all CpG sites in the naked DNA (Fig. 1C and 4D), indicating that the effect was not due to their individual DNA sequence specificity. The methylation level within the marginal region of both nucleosomes was summarized in Fig. 5C, showing that removal of

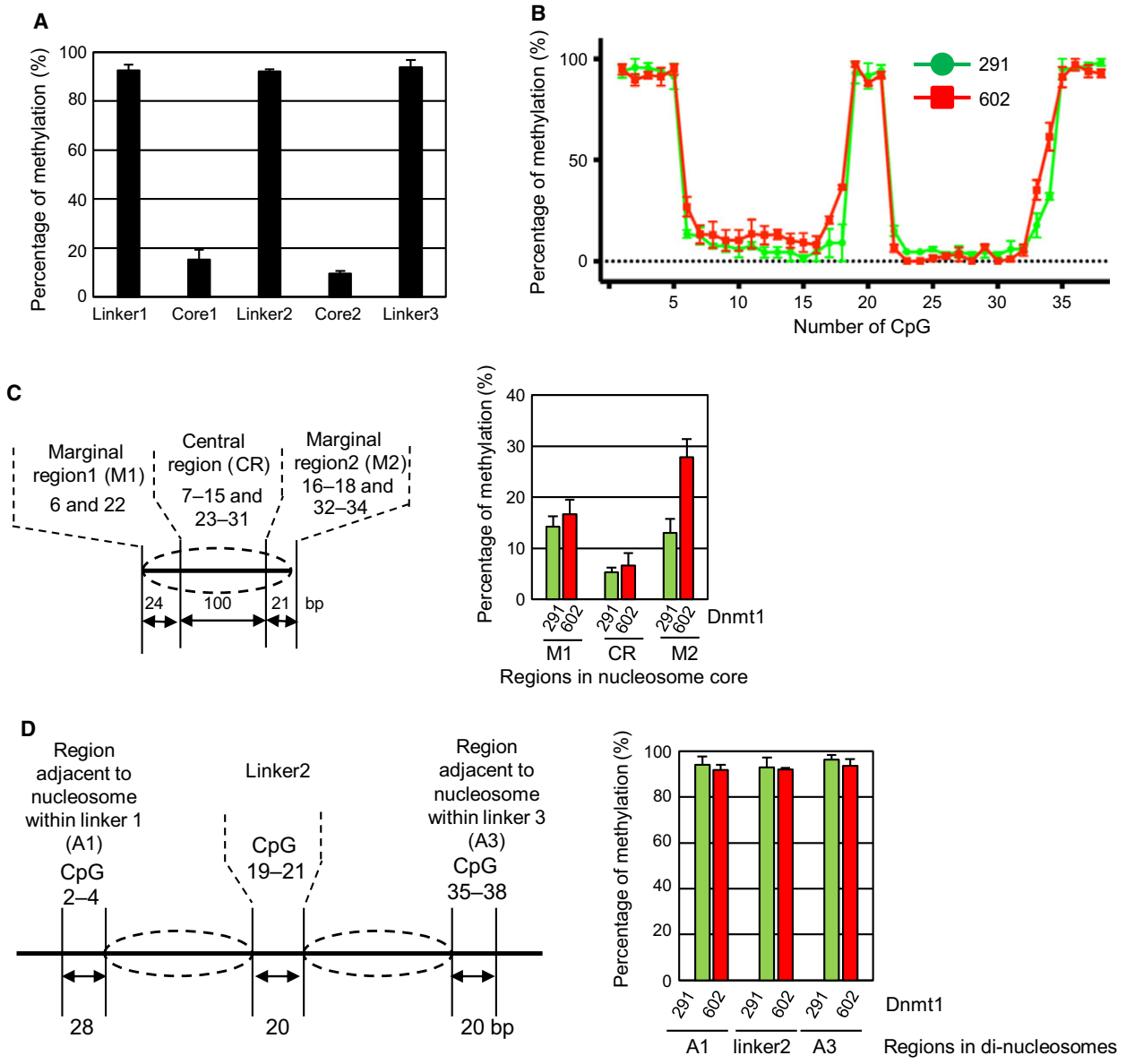

Fig. 5. Removal of RFTS increases DNA methylation at nucleosome entry/exit sites. (A) Region-specific methylation in nucleosomes by Dnmt1 602. Bar plot shows percentage of methylation as average of three independent experiments, shown in Figs 4D and S4. (B) Single-base analysis of DNA methylation. The percentage of DNA methylation in each CpG was plotted to the DNA sequence. Dinucleosomes were methylated with Dnmt1 291 (green line) or Dnmt1 602 (red line). The percentage ± SD (n = 3) is shown. The data are derived from Figs 2D and S2 (Dnmt1 291), Figs 4D and S4 (Dnmt1 602). (C) DNA methylation within core particles. Core region was divided into three regions, marginal region (M1 and M2), and central region (CR) (left panel). The percentage of methylation in the regions (n = 3) are shown in a bar plot (right panel). The percentages of Dnmt1 291 and Dnmt1 602 are shown in green and red, respectively. The data were taken from Figs 2D and S2 (Dnmt1 291), Figs 4D and S4 (Dnmt1 602). (D) Methylation in regions close to nucleosome cores. Region adjacent to nucleosome cores (A1 and A3) were defined as described in left panel. The region between two nucleosomes is designated as linker 2 in left panel. Average ± SD of methylation in the regions was calculated from three independent experiments (right panel) (Dnmt1 291; Figs 2D and S2, Dnmt1 602; Figs 4D and S4).

RFTS increased the methylation in the M2 marginal region by around twofold). Within the M2 regions, increased methylation was restricted to the two outermost CpG sites (17, 18, 33, and 34), which are 12 and 18 bp apart from the nucleosome exit. No change was seen at CpGs 16 and 32 in the M2 region or CpG

22 within the M1 region which are 24 and 22 bp away from the core, respectively. In contrast, toward naked DNA regions (A1, linker2, and A3) in nucleosomes, Dnmt1 291 and 602 showed similar DNA methylation activity (Fig. 5D). Thus, RFTS obstructs Dnmt1 activity toward CpG sites within the entry/exit region of the nucleosome core which are subject to spontaneous unwrapping described as 'breathing' [20,21]. In addition, the methylation pattern in the two consecutive nucleosomes was similar (Fig. 5B), indicating that methylation activity at entry/exit sites was not affected by the length of the adjacent linker DNA.

RFTS-dependent repression of Dnmt1 activity by histone N-terminal region

Because the histone H3 N terminus is protruding at 3 bp distant from nucleosome entry/exit sites, we next addressed the possibility that histone tails directly inhibit the activity of Dnmt1 [22]. The activity of Dnmt1 291 toward 42-bp oligonucleotides containing 12 hemimethylated CpG sites (42 bp/12hmCpG) (Table S2) was repressed by histone tail peptides. Histone H3 (1–30) repressed the activity of Dnmt1 291 with a half maximal inhibitory concentration (IC50) of approximately 2 μM (Fig. 6A and Table S1) while it did not affect the bacterial DNA methyltransferase M. SssI (Fig. 6B). The activity of Dnmt1 FL was also reduced by H3 (1–30), but the effect was slightly weaker compared to Dnmt1 291 (Fig. 6C), suggesting that the N-terminal region (1–290 aa) of Dnmt1 did not contribute to repression.

Substrate binding to Dnmt1 can be monitored by using an oligonucleotide in which the target cytosine in a CpG site is substituted with fluorocytosine (F-oligo). This substrate is covalently cross-linked upon binding the catalytic center and the cross-linked product can be monitored by slower migration of Dnmt1 in SDS/PAGE [23,24]. The formation of the reaction intermediate was reduced by adding H3 (1–30) to Dnmt1 291 (Fig. 6D). As the RFTS domain of Dnmt1 (291–602) bound to the histone H3 tail and RFTS removal derepressed methylation in the marginal region of nucleosomes, we next examined the effect of H3 (1–30) on the activity of Dnmt1 602. Dnmt1 602 activity was not suppressed by H3 (1–30), and rather slightly stimulated at low concentration (Fig. 6E). Substrate binding to Dnmt1 602 as monitored by using F-oligo was not repressed by H3 (1–30) (Fig. 6D). These results indicate that the inhibitory effect of histone tails on Dnmt1 activity is not due to capture of negatively charged DNA substrates by basic peptides but rather caused by interaction with RFTS.

Dnmt1 291 repression is modulated by histone tail post-translational modifications

It has been reported that Dnmt1 binds to histone deacetylases [25–27] as well as histone H3 methyltransferases SUV39H1 and G9a [28,29]. Furthermore, Dnmt1 binds to HP1 and Uhrf1 (Np95) which recognize K9 methylated H3 and release RFTS-dependent inhibition [28,30]. We therefore examined whether post-translational modifications on H3 (1–30) can change the inhibitory effect of the H3 peptide. Acetylation of lysine residues in H3 (1–30), H3 (1–30)ac, abolished the repressive effect on Dnmt1 291 activity in the tested concentration range (Fig. 7A). In contrast, H3 (1–30) K9me3 repressed Dnmt1 291 activity, although to a lower extent than the unmodified peptide (Fig. 7B). Thus, histones and their modifications can modulate the activity of Dnmt1. In consistency with the effect on Dnmt1 activity, RFTS did not bind to H3 (1–30) ac, but to H3 (1–30)K9me3 (Fig. 7C).

Dnmt1 processively methylates hemimethylated DNA, whereas unmethylated substrate is modified distributively [7]. We next tested whether the observed repression by H3 tail was due to specific inhibition of the processive reaction. We therefore used 42-bp oligonucleotides as substrate in which only one CpG site was hemimethylated (42 bp/1hmCpG) (Table S2). Toward 42 bp/1hmCpG, the activity of Dnmt1 291 was also repressed (Fig. 7D), suggesting that processive and nonprocessive methylation were equally affected by H3 (1–30).

To further narrow down histone tail regions required for inhibition, we prepared truncated H3 peptides. H3 (10–30) did not inhibit Dnmt1 291 activity, while H3 (1–20) showed a biphasic effect (Fig. 8A). Dnmt1 291 activity was slightly stimulated at less than 10 μM H3 (1–20), but the stimulatory effect was lost at higher concentration. H3 (5–30) or (1–25) repressed Dnmt1 291 activity, but the effect was milder than H3 (1–30). Loss of inhibition with truncated peptides suggests that a large binding interface is needed for Dnmt1 repression by histone H3.

A peptide (H3 rev) in which the amino acid sequence of H3 was inverted (Table S1) inhibited Dnmt1 activity with similar potency (Fig. 8B), suggesting that not the amino acid sequence but the total charge of the peptide is essential for the repression. We further examined whether the repressive effect is dependent on amino acid sequence. H4 (1–30), with a pI similar to H3 (10–30) (Table S1), inhibited the activity of Dnmt1 291 (Fig. 8C), however, the repressive effect was weaker than H3 (1–30) (compare to

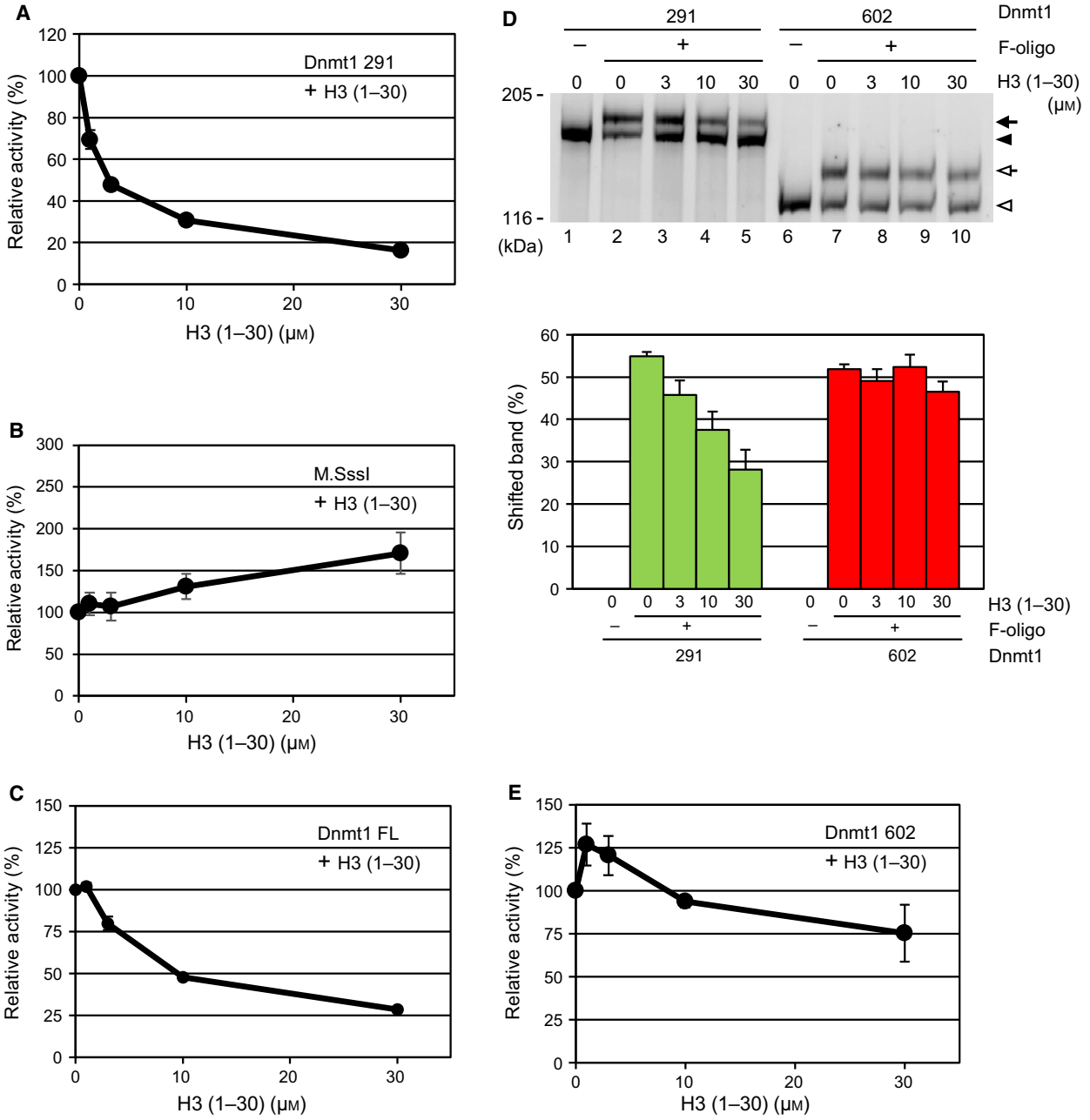

Fig. 6. Histone H3 tail negatively regulates the activity of Dnmt1 291 but not Dnmt1 602. Effect of histone H3 (1–30) on the DNA methylation activity of Dnmt1 291 (A), M. SssI (B), Dnmt1 FL (C), and Dnmt1 602 (E). Activity without peptide was taken as 100%, and the relative activity is shown. Activity was measured by using oligonucleotides 42 bp/12hmCpG, and shown as average ± SD ($n = 3$). (D) Monitoring the intermediate step of the DNA methylation reaction. DNA methylation reaction of Dnmt1 291 and 602 was performed with F-oligonucleotide in the presence of 0 (lanes 2 and 7), 3 (lanes 3 and 8), 10 (lanes 4 and 9), and 30 μM histone H3 (1–30) (lanes 5 and 10), or without histone F-oligo or peptide (lanes 1 and 6). Reaction products were separated with SDS/PAGE (upper panel). Bands of free Dnmt1 and DNA-bound Dnmt1 were shown arrows and arrowheads, respectively. The bands of Dnmt1 291 and Dnmt1 602 were indicated by closed and open marks, respectively. Average percentage of shifted bands from three independent experiments ± SD are shown in bar plot (lower panel).

Fig. 5A). Histone H2B (1–27) which has a lower pKa than H3 (10–30) (Table S1), did not inhibit the activity of Dnmt1 291 (Fig. 8D). In summary, histone tails can modulate Dnmt1 activity in a histone molecule-dependent manner, and their inhibitory effect is influenced by post-translational modifications.

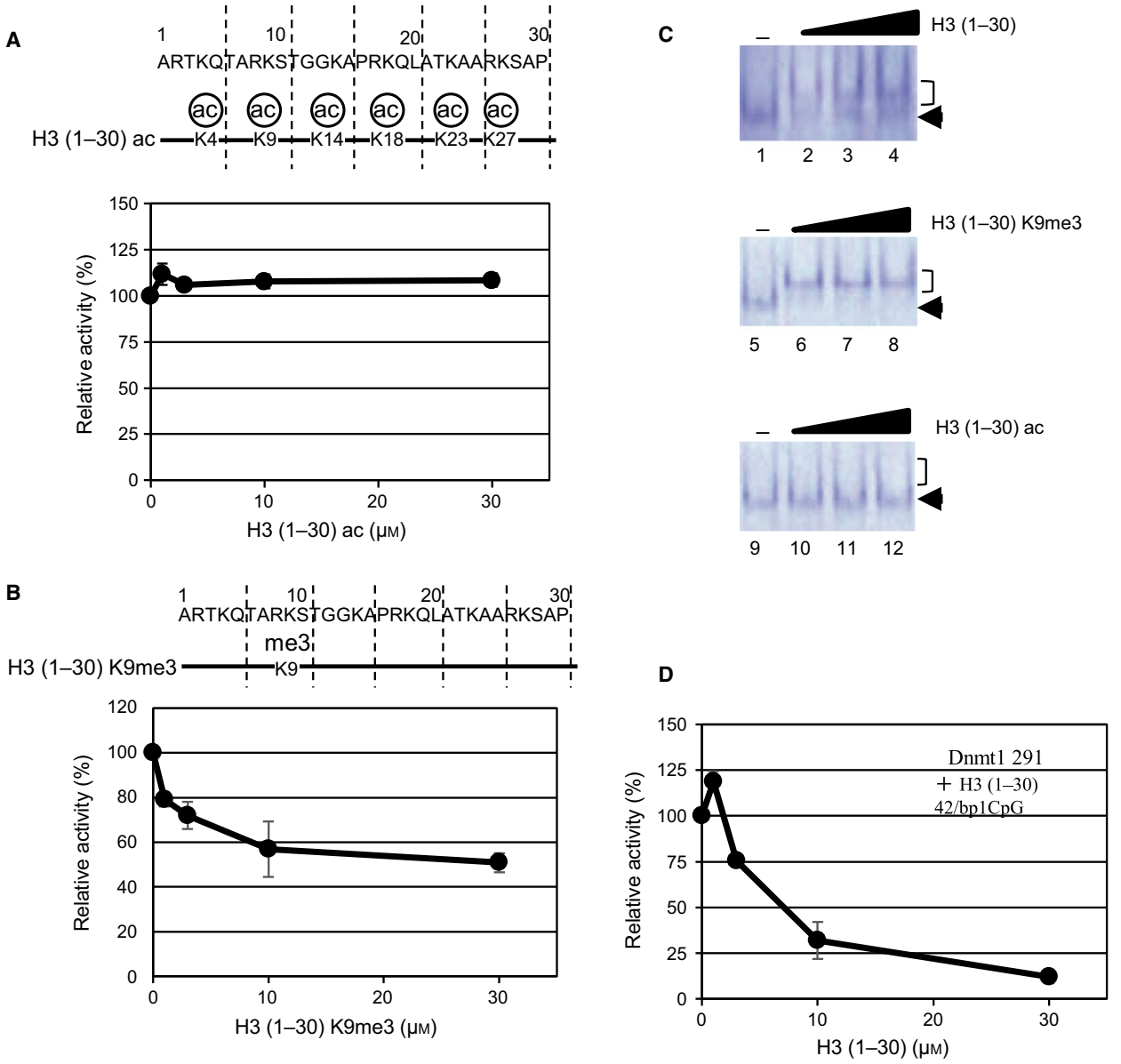

Fig. 7. Detailed analysis of repression properties of Dnmt1 291. (A) Acetylation released the repression by H3 (1–30). Acetylation sites (ac) are shown in upper panel. (B) Repression of Dnmt1 291 by H3 (1–30) K9me3. Trimethylation site (me3) is shown in upper panel. The effect of modified H3 (1–30) on Dnmt1 291 activity was determined as described in Fig. 6, by using 42 bp/12hmCpG as substrates. (C) The effect of post-translational modifications on the interaction between RFTS and H3 (1–30). The interaction was monitored as in Fig. 4A. Recombinant GST-tagged Dnmt1 (291–601) was mixed with 5.6× (lanes 2 and 6 and 10), 17× (lanes 3, 7 and 11), and 56× (lanes 4, 8 and 12) molar excess of unmodified histone H3 (lanes 1–4) histone H3 (1–30)K9me3 (lanes 5–8) or histone H3 (1–30)ac (lanes 9–12). (D) Effect of histone H3 (1–30) on DNA methylation activity of Dnmt1 291 toward oligonucleotide 42 bp/1hmCpG, was examined. The activity in the absence of the peptide was taken as 100%, and the average ± SD (n = 3) is shown.

Discussion

Dnmt1 activity toward nucleosomes reconstituted with unmethylated or hemimethylated DNA has been reported [14–17]. Schrader *et al.* examined Dnmt1 activity toward nucleosomes including hemimethylated DNA, and reported an overall repressive effect, however, not resolved by nucleosome regions [17]. As Dnmt1 switches from distributive to processive methylation when presented with hemimethylated substrate, we analyzed Dnmt1 maintenance methylation activity at single CpG resolution on dinucleosomes containing hemimethylated DNA [7]. We found that Dnmt1

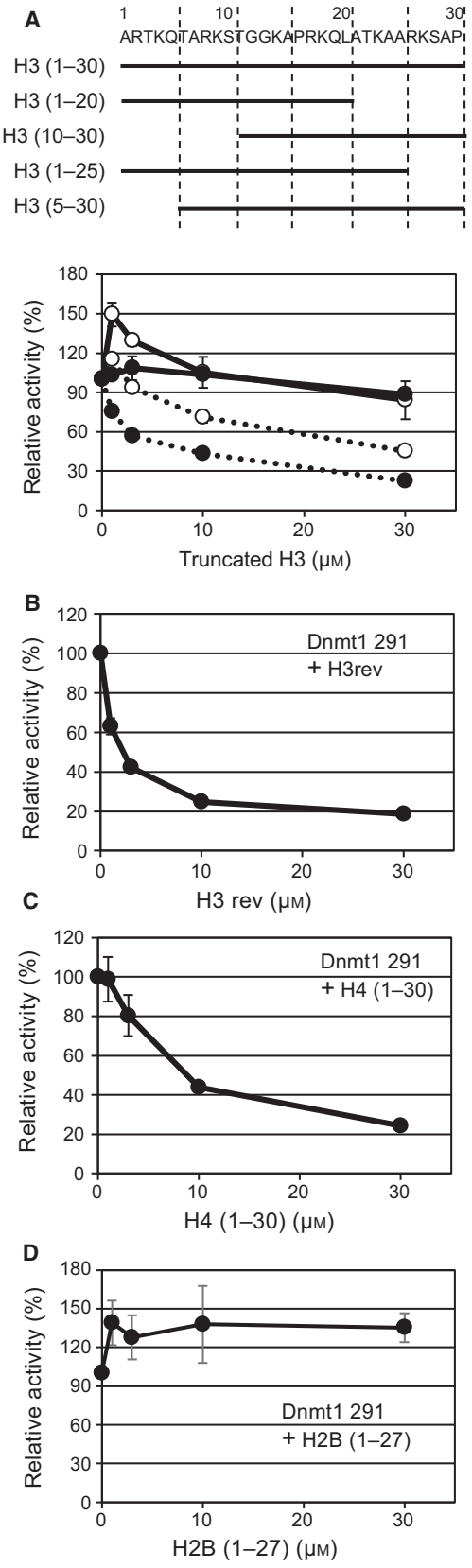

maintenance methylation activity was blocked at CpGs in nucleosome cores and the repression was partially released by removal of the RFTS domain.

The RFTS guides Dnmt1 to replication foci in S-phase [31] and increases activation energy by intramolecular binding to the catalytic domain via hydrogen bonds [9,23]. The interaction between RFTS and the catalytic domain of Dnmt1 is released by interaction with the SRA domain of Uhrf1 [23], and Uhrf1 is crucial for DNA methylation [30]. Although several roles of RFTS in Dnmt1 function have been reported, its function in a nucleosomal context remains to be elucidated. In the present study, we observed that RFTS obstructs Dnmt1 access to nucleosome entry/exit sites. We also found that RFTS is directly bound by the N terminus of histone H3 and that this interaction inhibits Dnmt1 catalytic activity, potentially by stabilizing RFTS-dependent autoinhibition. Thus, RFTS regulates Dnmt1 activity not only by intramolecular interaction [9,32] but it also mediates Dnmt1 regulation by histones. Furthermore, as free, modified histones not incorporated in chromatin are observed in the nucleus [33], the repression of Dnmt1 by histone tails could not be limited to nucleosome structures.

In contrast to Dnmt1, *de novo* DNA methyltransferase Dnmt3a, as well as the Dnmt3a/Dnmt3L complex methylate linker DNA preferentially in a nucleosomal context [34,35]. The histone H3 tail stimulates the enzymatic activity of Dnmt3a *in vitro* and stimulation was abrogated by H3K4 methylation [35–37]. We showed that maintenance methylation by Dnmt1 is inhibited by histone H3, H3 methylated at lysine 9 and H4, and that the inhibitory effect of histone H3 is released by acetylation. Thus, *de novo* methyltransferase Dnmt3a and maintenance DNA methyltransferase Dnmt1 are oppositely regulated by unmodified histone H3.

We observed that H3 peptide with inverted amino acid sequence inhibited Dnmt1 with similar potency as the native H3 tail. Therefore, the polykationic nature of the peptide might be more important for inhibition than the peptide structure, possibly affecting protein or DNA conformation.

Fig. 8. Effect of truncated H3 tail. H3 rev, H4 tail, and H2B tail on Dnmt1 291 activity. The effect of H3 (1–20) (open circles with solid line), (1–25) (open circles with broken line), (5–30) (closed circles with broken line), and (10–30) (closed circles with solid line) (A), H3 rev (B), H4 (1–30) (C), and H2B (1–27) (D), (amino acid sequences are shown in Table S1) on Dnmt1 291 activity toward 42 bp/12hmCpG was verified as in Fig. 5. The relative activity was shown as average ± SD (n = 3).

In conclusion, this study shows a role of RFTS in regulating Dnmt1 function in a nucleosomal context and in mediating inhibition of Dnmt1 by histone tails. Future investigation should address the interaction between histone modifications and Dnmt1 to elucidate the regulation of DNA maintenance methylation.

Materials and methods

Preparation of hemimethylated DNA

Hemimethylated DNA was prepared basically as described by Hermann *et al.* [38] but including a purification step to reduce contamination by fully methylated DNA in the product. The 601.2 sequence (Fig. S1) was amplified with primer A and B, and then 2 mg of DNA was methylated with 0.2 mg of M. SssI (NEB). Methylated DNA (2 mg) was treated with 3 μg of λ exo at 37 °C for 2 h to remove the lower strand, and then purified. The purification was performed using 6% acrylamide disk gel in Mini Prep Cell (BioRad, Tokyo, Japan) with 1 watt. The size of eluted DNA was monitored with 5% native PAGE in 1× TBE buffer. The fractions containing only single-stranded DNA were collected, annealed with primer C by incubation at 95 °C for 2 min, and cooled down to 37 °C with a 15 min linear gradient. The annealed DNA (3 μg) was mixed with 1.3 μg of T4 polymerase in a buffer containing 7 mM $MgCl_2$, 15 mM $(NH_4)_2SO_4$, 0.5 mM DTT, 0.1 mM EDTA, 0.5 mM dNTP, and 50 mM Tris-HCl, pH8.5, and incubated 37 °C for 5 min to fill in the lower strand. The filled in DNA was digested with *Hin*dIII and *Bam*HI and the product was purified with 9% acrylamide disk gel in Mini Prep Cell. The preparation steps were summarized in Fig. 1A.

Preparation of recombinant proteins and peptides

For truncated Dnmt1, Sf9 insect cells were infected with baculoviruses harboring cDNA of Dnmt1 which encodes amino acids 291–1620 or 602–1620. The expressed Dnmt1 was purified as described by Takeshita *et al.* [9]. For GST-Dnmt1 (291–601), cDNAs corresponding to GST and the Dnmt1 fragment were sequentially subcloned into an expression plasmid, pFASTBAC1 (Invitrogen, Tokyo, Japan) in frame, and baculovirus was prepared as described [6]. Sf9 cells infected with the virus were suspended in buffer A (0.3 M NaCl, 0.3% (w/v) Nikkol (Nikko Chemicals, Tokyo, Japan), 3 mM $MgCl_2$, 1 M sucrose, 5 mM β-mercaptoethanol, 1/2000 (v/v) protease inhibitor cocktails (PI) (Nacalai Tesque, Kyoto, Japan), 20 mM Tris-HCl, pH7.4), and centrifuged at 10 000 ***g*** for 5 min. Supernatant was purified with glutathione Sepharose (GE Healthcare, Tokyo, Japan). For GST or GST-Dnmt1 (1–118), pGEX or pGEX with the respective cDNA inserts were transformed into BL21, and cultured at 18 °C. GST or GST-Dnmt1 (1–118) was purified as described for GST-Dnmt1 (1–291).

cDNA coding for T4 polymerase was amplified by PCR from T4 phage DNA and subcloned in frame into pET30a plasmids via *Bam*H1 and *Sal*I sites. The expression plasmid was transformed into BL21 RIL, and its expression was induced by adding 0.5 mM IPTG at 18 °C. Bacteria were suspended in buffer B (0.5 M NaCl, 0.1% (w/v) Triton X-100, 5 mM β-mercaptoethanol, 1/2000 (v/v) PI, 10 mM Tris-HCl, pH 7.4), and sonicated. After centrifugation (10 000 ***g*** for 10 min), the supernatant was loaded onto HisAccept (Nacalai Tesque). The column was washed with buffer B containing 10 mM imidazole, and eluted with buffer B containing 250 mM imidazole. The eluate was diluted 10 times with 10 mM Tris-HCl, pH 7.4, loaded onto a HitrapQ FF column (GE Healthcare), and eluted with a gradient (50–800 mM NaCl, 10 mM Tris-HCl, pH 7.4, 0.1% (w/v) Triton X-100, 1/1000 (v/v) PI, 5 mM β-mercaptoethanol). For preparing expression vector of λ exonuclease (λ exo), cDNA was cloned into pBAD vector with a His-tag at the N terminus of λ exo. The expression vector was transformed into ER1821 and expression was induced by 0.2% (v/v) arabinose for 16 h at 18 °C. Bacteria were suspended in buffer C (0.1% (w/v) Triton X-100, 5 mM β-mercaptoethanol, 0.3 M NaCl, 1 mM $MgCl_2$, 10 mM Tris-HCl, pH 7.4), and sonicated. After centrifugation (10 000 ***g*** for 10 min), the supernatant was loaded onto HisAccept. The column was washed with buffer C containing 10 mM imidazole, and eluted with buffer C containing 250 mM imidazole. Protein concentration was determined by bicinchoninic acid assay (Millipore, Tokyo, Japan). Recombinant histones were expressed and purified as described, and histone octamer was reconstituted as described by Luger *et al.* [39]. Modified and unmodified histone H3 peptides were synthesized and purified as described by Kawakami *et al.* [40]. Histone (1–27) was provided from Scrum Inc. (Tokyo, Japan).

Reconstitution of nucleosomes

Dinucleosomes were prepared and purified as described by Mishima *et al.* [41]. Briefly, histone octamers and DNA were mixed in buffer containing 2 M KCl, and salt concentration was gradually reduced by dialysis. After reconstitution, contaminating free DNA was removed by ultracentrifugation with a glycerol gradient. The nucleosome concentration was determined via absorbance at 260 nm.

Enzymatic digestion of reconstituted nucleosomes

Nucleosomes (35 ng of DNA) were digested with either *Alu*I (5 units) or *Sca*I (6 units) as described elsewhere [41]. Nucleosomes (35 ng of DNA) were treated with indicated

concentration of micrococcal nuclease, as described elsewhere [41].

Gel shift assay

GST-Dnmt1 (291–601), GST-Dnmt1 (1–118), or GST (180 nM) were mixed with 0–10 μM of amino terminal histone H3 peptide in buffer containing 0.01 (w/v) Tween20, 50 mM NaCl, 15% (v/v) glycerol, 20 mM Tris-HCl, pH 7.5 and incubated on ice for 30 min. The mixture was separated in 6% native PAGE. Proteins were detected with Coomassie Brillian Blue staining.

DNA methylation assay

Radioisotope-dependent assay of steady state methylation was performed as described by Takeshita *et al.* [9]. Briefly, annealed DNA (100 nM) was methylated with Dnmt1 (2 nM), in the presence of 2.2 μM [^{3}H]-SAM (PerkinElmer Life Sciences, Yokohama, Japan) in 25 μL of buffer F (5 mM EDTA, 2.7 M glycerol, 0.2 mM DTT, 0.2 mM phenylmethylsulfonyl fluoride, and 20 mM Tris-HCl, 7.4), at 37 °C for 1 h. Radioactivity incorporated in DNA was measured by liquid scintillation counter, as described by Takeshita [9].

For sodium bisulfite (BS) sequence analysis, 1.4 nM dinucleosomes or naked DNA were methylated with 30 nM of the indicated Dnmt1 versions, under conditions as described above for the methylation assay. To monitor the nucleosome deposition, 0.1 Unit·μL^{-1} of bacterial DNA methyltransferase M. AluI (NEB) was added in the reaction mixture. An aliquot of the reaction mixture was treated with Epitect bisulfite kit (Qiagen, Tokyo, Japan). The bisulfite-treated DNA was amplified by PCR with primers (SBS upper sd Fwd and SBS upper sd Rev, or SBS lower sd Fwd and SBS lower sd Rev) (Table S2). The amplified DNA was subcloned into pBlueScriptII and its sequence was determined by ABI 3100 DNA sequencer. CpG methylation was analyzed using QUMA [42].

F-oligo binding to Dnmt1

The two complementary oligonucleotides (20 bp/1CpG-F sense M and 20 bp/1CpG-antisense in Table S1) were annealed, and the annealed oligonucleotides (200 nM) were methylated with full-length or truncated Dnmt1 (80 nM), under the same conditions as for measuring methylation activity. After incubation at 37 °C for 1 h, the reaction mixtures were separated by 7% SDS/PAGE. Proteins were stained with Lumitein (Biotium, Inc, CA, USA), and bands were detected with a fluoro-imager, FLA9500, as described by Mishima *et al.* [43]. The percentage of shifted Dnmt1 over input Dnmt1 was calculated.

Acknowledgements

We thank Dr Shoji Tajima for preparing several expression vectors, and for critical discussions. We also acknowledge Ms Kaori Tada, Keiko Shinohara, and Junko Abe for protein purification. This work was, in part, supported by JSPS KAKENHI Grant Number 15K14418 (IS), and by AMED-CREST from Japan Agency for Medical Research and Development, AMED. This work was performed in part under the Cooperative Research Program of Institute for Protein Research, Osaka University, CR-1703.

Author contributions

IS conceived and supervised the study; LB, ST, JO, MS, and IS designed experiments; YM, LB, TK, KA, SO, ST, and HH performed experiments; AS and MW contributed to the final version of the manuscript; IS and LB wrote the manuscript.

Conflict of Interest

The authors declare no conflict of interest associated with this manuscript.

References

1 Jones PA (2012) Functions of DNA methylation: islands, start sites, gene bodies and beyond. *Nat Rev Genet* **13**, 484–492.
2 Bestor TH (2000) The DNA methyltransferases of mammals. *Hum Mol Genet* **9**, 2395–2402.
3 von Meyenn F, Iurlaro M, Habibi E, Liu NQ, Salehzadeh-Yazdi A, Santos F, Petrini E, Milagre I, Yu M, Xie Z *et al.* (2016) Impairment of DNA methylation maintenance is the main cause of global demethylation in naive embryonic stem cells. *Mol Cell* **62**, 848–861.
4 Chen T, Hevi S, Gay F, Tsujimoto N, He T, Zhang B, Ueda Y & Li E (2007) Complete inactivation of DNMT1 leads to mitotic catastrophe in human cancer cells. *Nat Genet* **39**, 391–396.
5 Elliott EN, Sheaffer KL, Schug J, Stappenbeck TS & Kaestner KH (2015) Dnmt1 is essential to maintain progenitors in the perinatal intestinal epithelium. *Development* **142**, 2163–2172.
6 Vilkaitis G, Suetake I, Klimasauskas S & Tajima S (2005) Processive methylation of hemimethylated CpG sites by mouse Dnmt1 DNA methyltransferase. *J Biol Chem* **280**, 64–72.
7 Goyal R, Reinhardt R & Jeltsch A (2006) Accuracy of DNA methylation pattern preservation by the Dnmt1 methyltransferase. *Nucleic Acids Res* **34**, 1182–1188.

8 Li E, Bestor TH & Jaenisch R (1992) Targeted mutation of the DNA methyltransferase gene results in embryonic lethality. *Cell* **69**, 915–926.
9 Takeshita K, Suetake I, Yamashita E, Suga M, Narita H, Nakagawa A & Tajima S (2011) Structural insight into maintenance methylation by mouse DNA methyltransferase 1 (Dnmt1). *Proc Natl Acad Sci U S A* **108**, 9055–9059.
10 Zhang Z-M, Liu S, Lin K, Luo Y, Perry JJ, Wang Y & Song J (2015) Crystal structure of human DNA methyltransferase 1. *J Mol Biol* **427**, 2520–2531.
11 Qin W, Wolf P, Liu N, Link S, Smets M, La Mastra F, Forné I, Pichler G, Hörl D, Fellinger K *et al.* (2015) DNA methylation requires a DNMT1 ubiquitin interacting motif (UIM) and histone ubiquitination. *Cell Res* **25**, 1–19.
12 Nishiyama A, Yamaguchi L, Sharif J, Johmura Y, Kawamura T, Nakanishi K, Shimamura S, Arita K, Kodama T, Ishikawa F *et al.* (2013) Uhrf1-dependent H3K23 ubiquitylation couples maintenance DNA methylation and replication. *Nature* **502**, 249–253.
13 Misaki T, Yamaguchi L, Sun J, Orii M, Nishiyama A & Nakanishi M (2016) The replication foci targeting sequence (RFTS) of DNMT1 functions as a potent histone H3 binding domain regulated by autoinhibition. *Biochem Biophys Res Commun* **470**, 741–747.
14 Robertson AK, Geiman TM, Sankpal UT, Hager GL & Robertson KD (2004) Effects of chromatin structure on the enzymatic and DNA binding functions of DNA methyltransferases DNMT1 and Dnmt3a in vitro. *Biochem Biophys Res Commun* **322**, 110–118.
15 Gowher H, Stockdale CJ, Goyal R, Ferreira H, Owen-Hughes T & Jeltsch A (2005) De novo methylation of nucleosomal DNA by the mammalian Dnmt1 and Dnmt3A DNA methyltransferases. *Biochemistry* **44**, 9899–9904.
16 Okuwaki M & Verreault A (2004) Maintenance DNA methylation of nucleosome core particles. *J Biol Chem* **279**, 2904–2912.
17 Schrader A, Gross T, Thalhammer V & Langst G (2015) Characterization of Dnmt1 binding and DNA methylation on nucleosomes and nucleosomal arrays. *PLoS One* **10**, e0140076.
18 Garvilles RG, Hasegawa T, Kimura H, Sharif J, Muto M, Koseki H, Takahashi S, Suetake I & Tajima S (2015) Dual functions of the RFTS domain of dnmt1 in replication-coupled DNA methylation and in protection of the genome from aberrant methylation. *PLoS One* **10**, e0137509.
19 Portela A, Liz J, Nogales V, Setién F, Villanueva A & Esteller M (2013) DNA methylation determines nucleosome occupancy in the 5'-CpG islands of tumor suppressor genes. *Oncogene* **32**, 5421–5428.
20 Polach KJ & Widom J (1995) Mechanism of protein access to specific DNA sequences in chromatin: a dynamic equilibrium model for gene regulation. *J Mol Biol* **254**, 130–149.
21 Li G & Widom J (2004) Nucleosomes facilitate their own invasion. *Nat Struct Mol Biol* **11**, 763–769.
22 Luger K, Mäder AW, Richmond RK, Sargent DF & Richmond TJ (1997) Crystal structure of the nucleosome core particle at 2.8 A resolution. *Nature* **389**, 251–260.
23 Berkyurek AC, Suetake I, Arita K, Takeshita K, Nakagawa A, Shirakawa M & Tajima S (2014) The DNA methyltransferase Dnmt1 directly interacts with the SET and RING finger-associated (SRA) domain of the multifunctional protein Uhrf1 to facilitate accession of the catalytic center to hemi-methylated DNA. *J Biol Chem* **289**, 379–386.
24 Brank AS, Van Bemmel DM & Christman JK (2002) Optimization of baculovirus-mediated expression and purification of hexahistidine-tagged murine DNA (cytosine-C5)-methyltransferase-1 in Spodoptera frugiperda 9 cells. *Protein Expr Purif* **25**, 31–40.
25 Fuks F, Burgers WA, Brehm A, Hughes-Davies L & Kouzarides T (2000) DNA methyltransferase Dnmt1 associates with histone deacetylase activity. *Nat Genet* **24**, 88–91.
26 Rountree MR, Bachman KE & Baylin SB (2000) DNMT1 binds HDAC2 and a new co-repressor, DMAP1, to form a complex at replication foci. *Nat Genet* **25**, 269–277.
27 Robertson KD, Ait-Si-Ali S, Yokochi T, Wade PA, Jones PL & Wolffe AP (2000) DNMT1 forms a complex with Rb, E2F1 and HDAC1 and represses transcription from E2F-responsive promoters. *Nat Genet* **25**, 338–342.
28 Smallwood A, Estève PO, Pradhan S & Carey M (2007) Functional cooperation between HP1 and DNMT1 mediates gene silencing. *Genes Dev* **21**, 1169–1178.
29 Fuks F, Hurd PJ, Deplus R & Kouzarides T (2003) The DNA methyltransferases associate with HP1 and the SUV39H1 histone methyltransferase. *Nucleic Acids Res* **31**, 2305–2312.
30 Sharif J, Muto M, Takebayashi S, Suetake I, Iwamatsu A, Endo TA, Shinga J, Mizutani-Koseki Y, Toyoda T, Okamura K *et al.* (2007) The SRA protein Np95 mediates epigenetic inheritance by recruiting Dnmt1 to methylated DNA. *Nature* **450**, 908–912.
31 Leonhardt H, Page AW, Weier HU & Bestor TH (1992) A targeting sequence directs DNA methyltransferase to sites of DNA replication in mammalian nuclei. *Cell* **71**, 865–873.
32 Syeda F, Fagan RL, Wean M, Avvakumov GV, Walker JR, Xue S, Dhe-Paganon S & Brenner C (2012) The replication focus targeting sequence (RFTS) domain is a DNA-competitive inhibitor of Dnmt1. *J Biol Chem* **286**, 15344–15351.

33 Pinheiro I, Margueron R, Shukeir N, Eisold M, Fritzsch C, Richter FM, Mittler G, Genoud C, Goyama S, Kurokawa M *et al.* (2012) Prdm3 and Prdm16 are H3K9me1 methyltransferases required for mammalian heterochromatin integrity. *Cell* **150**, 948–960.
34 Takeshima H, Suetake I & Tajima S (2008) Mouse Dnmt3a preferentially methylates linker DNA and is inhibited by histone H1. *J Mol Biol* **383**, 810–821.
35 Zhang Y, Jurkowska R, Soeroes S, Rajavelu A, Dhayalan A, Bock I, Rathert P, Brandt O, Reinhardt R, Fischle W *et al.* (2010) Chromatin methylation activity of Dnmt3a and Dnmt3a/3L is guided by interaction of the ADD domain with the histone H3 tail. *Nucleic Acids Res* **38**, 4246–4253.
36 Li B-Z, Huang Z, Cui Q-Y, Song X-H, Du L, Jeltsch A, Chen P, Li G, Li E & Xu G-L (2011) Histone tails regulate DNA methylation by allosterically activating de novo methyltransferase. *Cell Res* **21**, 1172–1181.
37 Guo X, Wang L, Li J, Ding Z, Xiao J, Yin X, He S, Shi P, Dong L, Li G *et al.* (2015) Structural insight into autoinhibition and histone H3-induced activation of DNMT3A. *Nature* **517**, 640–644.
38 Hermann A, Goyal R & Jeltsch A (2004) The Dnmt1 DNA-(cytosine-C5)-methyltransferase methylates DNA processively with high preference for hemimethylated target sites. *J Biol Chem* **279**, 48350–48359.
39 Luger K, Rechsteiner TJ & Richmond TJ (1999) Expression and purification of recombinant histones and nucleosome reconstitution. *Methods Mol Biol* **119**, 1–16.
40 Kawakami T, Yoshikawa R, Fujiyoshi Y, Mishima Y, Hojo H, Tajima S & Suetake I (2015) Synthesis of histone proteins by CPE ligation using a recombinant peptide as the C-terminal building block. *J Biochem* **158**, 403–411.
41 Mishima Y, Watanabe M, Kawakami T, Jayasinghe CD, Otani J, Kikugawa Y, Shirakawa M, Kimura H, Nishimura O, Aimoto S *et al.* (2013) Hinge and chromoshadow of HP1α participate in recognition of K9 methylated histone H3 in nucleosomes. *J Mol Biol* **425**, 54–70.
42 Kumaki Y, Oda M & Okano M (2008) QUMA: quantification tool for methylation analysis. *Nucleic Acids Res* **36**, 170–175.
43 Mishima Y, Jayasinghe CD, Lu K, Otani J, Shirakawa M, Kawakami T, Kimura H, Hojo H, Carlton P, Tajima S *et al.* (2015) Nucleosome compaction facilitates HP1γ binding to methylated H3K9. *Nucleic Acids Res* **43**, 10200–10212.

Supporting information

Additional Supporting Information may be found online in the supporting information tab for this article:

Table S1. Amino acids sequence of H3 and H4 peptides.
Table S2. Oligonucleotides used for analyzing Dnmt1 activity.
Table S3. Oligonucleotide for PCR and fill-in reaction.
Fig. S1. Sequence of hemimethylated DNA.
Fig. S2. Reproducibility of Dnmt1 291 methylation activity.
Fig. S3. Nucleosome structure-dependent DNA methylation activity of Dnmt1 FL.
Fig. S4. Reproducibility of Dnmt1 602 methylation activity toward naked DNA or dinucleosomes.